Network upgrade exploiting multi band: S- or E-band?

Network upgrade exploiting multi band: S or E-band?

NICOLA SAMBO[1,*], BRUNO CORREIA[2], ANTONIO NAPOLI[3], JOÃO PEDRO[4,5], LEILY KIANI[6], PIERO CASTOLDI[1], AND VITTORIO CURRI[2]

[1] *Scuola Superiore Sant'Anna, Pisa, Italy.*
[2] *Politecnico di Torino, Torino, Italy.*
[3] *Infinera, Strategy, Architecture, and Engineering, Munich, Germany.*
[4] *Infinera Unipessoal Lda., Carnaxide, Portugal.*
[5] *Instituto de Telecomunicações, Instituto Superior Técnico, Lisboa, Portugal.*
[6] *Lawrence Livermore National Laboratory, California, USA.*
[*] *Corresponding author: nicola.sambo@santannapisa.it.*

Compiled May 23, 2023

Nowadays, the fiber spectrum is only partially exploited, i.e., mainly in the C-band and more recently in the C+L-band, where the fiber attenuation profile experiences the minimum. Thus, fiber communications technology – amplifiers, switching, transceivers, etc. – and networking solutions are mature for those spectrum bands. However, the continuous increase in traffic means that capacity saturation of the current infrastructure is looming. Taking advantage of the unused portions of the spectrum (e.g., S- and E-band) may be an efficient solution to accommodate an increase in traffic without installing new fibers. Research is thus investigating multi-band transmission and networking to evaluate and enable such network upgrades. Some issues need to be solved or taken into account, from the enabling technology (e.g., amplifiers in the S- or E-band are still under development) to physical layer effects previously neglected, such as the Stimulated Raman Scattering (SRS). SRS affects wideband-transmission, potentially degrading active channels. The contribution of this paper is the investigation of network upgrades for C+L-band systems. In particular, upgrades exploiting E- and S-band are compared taking into account each band capacity and the effects of SRS on both new and already deployed channels (in both the C- and L-band). A detailed analysis of the physical layer is provided, also in the presence of guard bands between previously exploited bands and the bands used for upgrade. By leveraging on the physical layer assessment, a networking analysis is carried on to evaluate the supported traffic increase and also the signal quality degradation due to SRS on active channels. The results suggest that upgrades to the E and S bands support a comparable increase in traffic. However, the exploitation of the E-band with 14 THz of guard band between C- and E-band may avoid detrimental effects to already active channels in C+L-band, suggesting this upgrade strategy can be the most effective of the two.

http://dx.doi.org/10.1364/ao.XX.XXXXXX

1. INTRODUCTION

The exploitation of bands beyond C and L (e.g., S- and E-band) is an effective solution to accommodate an increase in traffic without installing new fibers in the network [1–3]. Indeed, current deployed fibers are mainly used in the C-band and only in some cases in the L-band. Thus, in the near and medium term, network upgrades may exploit bands beyond C (and L), while in the long term, different solutions – such as the installation of several parallel fibers – could be adopted [4]. The first upgrades to the L-band have been carried out for example in [5]. In [6, 7], a preliminary network analysis on upgrades exploiting multi band was presented. In [8], the authors studied the impact of multi band on the capacity of networks equipped or not with regenerators (translucent and transparent networks, respectively), showing that the use of regenerators may significantly increase network capacity (e.g., via more extensive use of high-order modulation formats) at the expense of deploying more interfaces. However, the activation of an additional band in transparent networks results in a capacity equal to or larger than the one with a C-band-based translucent network and relying on fewer additional interfaces. Thus, the exploitation of other bands, such as S- and E-band, may permit operators to accommodate new traffic demands postponing investments. Multi-band transmission is also feasible considering that many of the currently deployed fibers do not present the absorption peak (occurring within the E-band) [3].

For the aforementioned reasons, the research community has

been investigating multi-band transmission and related enabling technology. In [9], transmission along L+C+S-band has been demonstrated for 40 Gb/s channels. Similarly, in [10], 40 Gb/s transmission over the S-band was demonstrated over installed fibers. Regarding the enabling technology, first of all, erbium doped fiber amplifiers (EDFA) mainly operate in C+L-band, not in the other bands. Amplifiers based on a thulium-doped fiber amplifier (TDFA) operating in S-band are commercially available [11, 12]. In the E-band, bismuth doped fiber amplifiers (BDFA) [13] or Nd^{3+} doped fiber amplifier (NDFA) [14] have been investigated. For what concerns wavelength switching, current commercial wavelength selective switches (WSS, e.g., Waveshaper [15]) operate up to C+L-band. Recently, a 1×2 WSS [16] operating in O-, S-, C- and L-band and a 47-port WSS [17] in O-, E-, S-, and C-band have been demonstrated. In [18], the authors investigate the challenges of amplification and WSS, and an optical amplifier is presented to mitigate the SRS effect: an EDFA/BDFA hybrid amplifier operating at 100 nm is proposed; then, the design for an LCoS-based 2×35 WSS operating over the 100 nm is shown; finally, an amplifier is presented that embeds an optical spectrum processor showing the equalization of WDM channels with the ability to limit the detrimental impact of SRS effect. In [19], ~~the authors investigate transceivers and assume in-phase/quadrature (I/Q) modulators designed for the C-band, demonstrating the operability of commercial transceivers optimized for C-band in multi-band networks.~~ the authors investigate transceivers showing that – in the case of modulators designed for the C-band – the modulators may present a wavelength-dependent I/Q imbalance when they operate beyond C; however, this imbalance can be compensated with digital signal processing, finally, demonstrating the operability of commercial transceivers optimized for C-band in multi-band networks.

Moreover, we have to consider that, in such a wideband transmission scenario, Stimulated Raman Scattering (SRS) [20] is highly relevant, as it generates a power transfer from higher to lower frequency channels. This may imply a degradation in quality of transmission (QoT) in the running channels in the C and L bands [2]. Such a physical effect has to be evaluated and considered in network upgrades. Indeed, when planning a network upgrade to S- or E-band, the impact of SRS on the running channels in the C+L-band should be accounted for. Because of SRS, some channels in C+L-band may experience a QoT below the forward error correction (FEC) threshold, thus requiring reconfigurations, such as changing them to a lower-order modulation format or re-routing them. The former may imply a bit rate reduction; thus, additional channels should be set in order to guarantee the original end-to-end capacity. Such aspect has not be deeply investigated in the literature in the context of networking studies. Indeed, although SRS is typically taken into account, the major part of the contributions (e.g., [2, 21–23]) focus on provisioning schemes or – in general – on resource allocation schemes, highlighting the increase of network capacity when exploiting multi band, rather than analyzing upgrading and operational issues, such as the degradation of already active channels when activating an additional band.

In this paper, network upgrade based on S- and E-band is analyzed starting from a C+L-band system. For network upgrades exploiting the E-band, we propose adopting an appropriate guard band (GB) between the C- and E-band. The ~~objective~~ purpose is to design the GB so that the impact of the E-band on traffic in the C- and L-band, due to SRS, is significantly reduced or even negligible. This avoids – at the expense of having fewer available channels – QoT degradation for the channels already operating in the C- and L-band, which is paramount to guarantee seamless upgrades. Being transparent lightpaths mostly impaired by Gaussian disturbances (nonlinear impairments – NLI – and Amplified Spontaneous Emission – ASE – noise), the generalized signal-to-noise ratio (GSNR) is adopted as a figure of merit to estimate the QoT when exploiting coherent technologies [24, 25]. A GB of 14 THz between the C+L-band and the E-band can minimize the impact of activation of the E-band on the C+L channels: indeed, it is shown that with GB = 14 THz the E-band introduces negligible cross-effects on the GSNR, i.e., $\leq$ 0.2 dB, supporting that the proposed multi-band solution enables a seamless upgrade of the C+L-band line system [6].

In this work, then, a network-wide performance assessment is used to compare both upgrade options – to the E- or to S-band – in terms of supported traffic increase and reconfigurations required on the active channels in the C+L-band. The results suggest that upgrading to the E-band with GB = 14 THz can be more effective, as it provides a comparable traffic increase compared to activating the S-band or the E-band with smaller GB, while limiting reconfigurations on the already active channels in the C+L-band.

2. NETWORK ABSTRACTION AND PHYSICAL LAYER ASSESSMENT

Figure 1 illustrates an optical network composed by several optical line systems (OLS), which today mainly exploit the C-band. Due to the already commercially available technology, the next step to increase network capacity is the L-band upgrade, also based on EDFA amplification. This upgrade can be performed at the amplification sites without the need of a new fiber deployment, which it might be either very expensive or not possible at all [3]. To increase the OLS capacity even further, two spectral bands, the E- and the S-band, can be used. In order to properly evaluate each upgrade scenario, it is crucial to accurately model the multi-band transmission, considering all frequency dependent parameters, for both fiber and amplifier. Fig. 2(a) presents the attenuation (dB/km) and chromatic dispersion (ps/nm/km) profiles while Fig. 2(b) presents the nonlinear coefficient ($W^{-1} \cdot km^{-1}$) for standard single-mode fiber (SSMF) for all spectral bands used in this work. Moreover, the GSNR has been shown to be a fast and accurate QoT estimation, even for wide bandwidth transmission. To use GSNR, defined by Eq. 1 for the i-th channel, as a metric for QoT evaluation, we quantify the ASE power, which considers the ASE noise generated by the amplifiers to calculate the optical signal-to-noise ratio (OSNR) defined by Eq. 2, and the nonlinear (NL) power, which considers the NLI generated during the fiber propagation and is used to calculate the nonlinear signal-to-noise ratio (SNR_{NL}) defined by Eq. 3 [25], in which $P_{S,i}$ is the i-th channel input power. The NLI is computed using the Generalized Gaussian Noise (GGN) model accounting for SRS [20]. Finally, in order to compute the GSNR for an entire path composed by several spans, we used a disaggregated [25] abstraction of the physical layer defined by Eq. 4, which depends on the GSNR of each span s belonging to the lightpath l.

$$\mathrm{GSNR}_i = \left(\mathrm{OSNR}_i^{-1} + \mathrm{SNR}_{\mathrm{NL},i}^{-1}\right)^{-1}, \quad \textbf{(1)}$$

$$\mathrm{OSNR}_i = \frac{P_{S,i}}{P_{\mathrm{ASE},i}}, \quad \textbf{(2)}$$

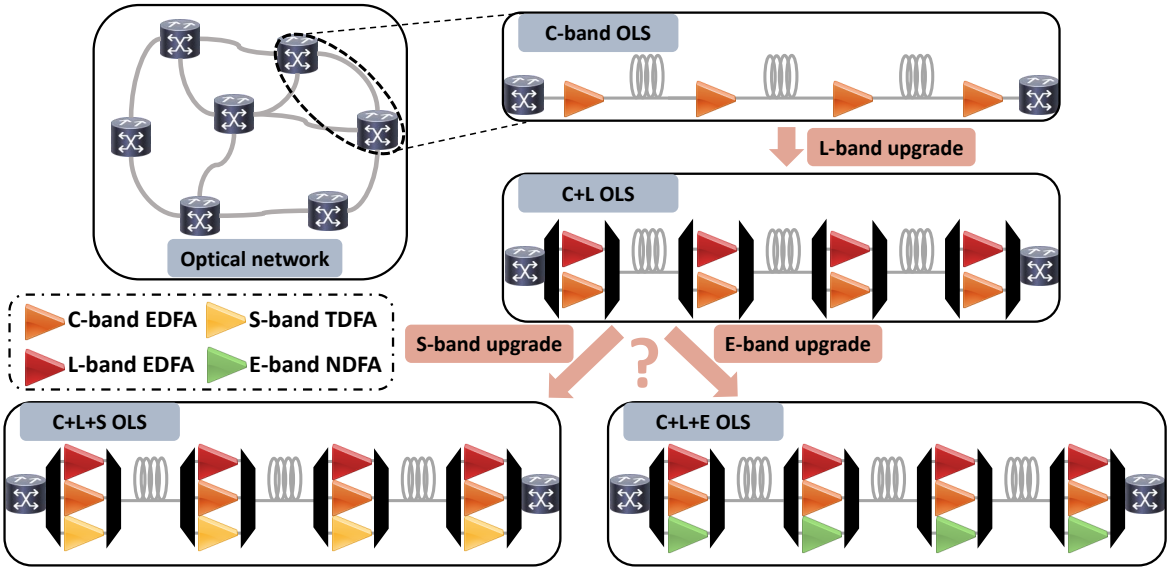

Fig. 1. Network and optical line system (OLS) abstraction for C-band and C+L-, C+L+S- and C+L+E-band upgrades.

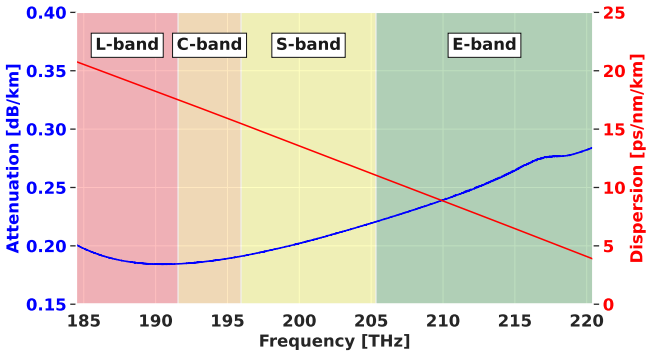

(a)

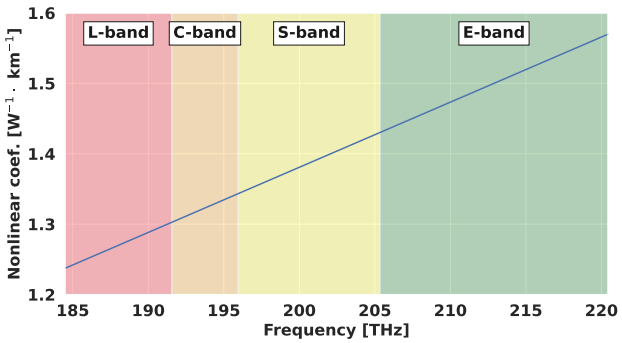

(b)

Fig. 2. (a) Fiber attenuation and chromatic dispersion profile and (b) Nonlinear coefficient of SSMF from L- to E-bands.

$$\mathrm{SNR}_{\mathrm{NL},i} = \frac{P_{S,i}}{P_{\mathrm{NLI},i}}, \tag{3}$$

$$\mathrm{GSNR}_{i,l} = \frac{1}{\sum_{s\in l}(\mathrm{GSNR}_{i,s})^{-1}} \tag{4}$$

~~The NLI is computed using the Generalized Gaussian Noise (GGN) model accounting for SRS~~ [20]. In this work, we compute the different number of channels under test (CUT) proportionally to the total number of channels in each band: 4, 7, 7 and 8 for C-, L-, S- and E-band, respectively. We assume optical channels operating with a symbol-rate of 64 GBaud and a 75 GHz WDM grid, capable of allocating a total of 92, 54, 125 and 146 channels in L-, C-, S- and E-band, respectively. We also evaluate the impact in using an additional 1.5 THz of bandwidth in E-band by adding 20 channels more, resulting in 166 channels in total. Moreover, we assumed the network is operated by C+L-band line systems relying on typical commercial EDFAs characterized by average noise figures of 4.2 dB and 4.7 dB for the C- and L-band, respectively. Note that we consider the frequency dependence of the amplifier characteristics. TDFA is assumed for S-band amplification, with average noise-figure of 6.5 dB [11]. We consider NDFA for the E-band as proposed in [14], with an average noise figure of 5.5 dB. Moreover, in this work we consider an ideal amplifier capable of recovering the input power at the end of each span. The entire physical layer analysis has been carried out with the open-source GNPy [26] tool.

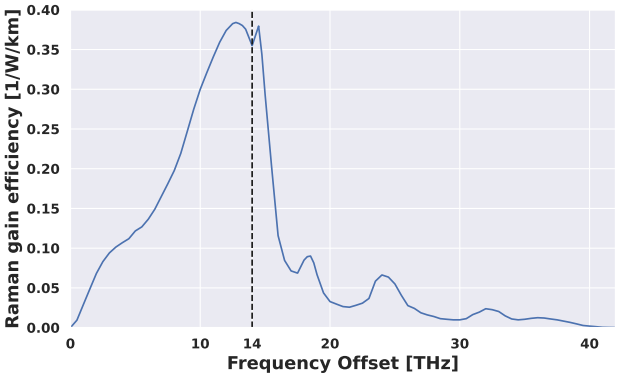

Fig. 3. Raman gain efficieny versus frequency offset for a SSMF.

As illustrated in Fig. 1, this work aims [at] an upgrade scenario after the deployment and utilization of a C+L-band system.

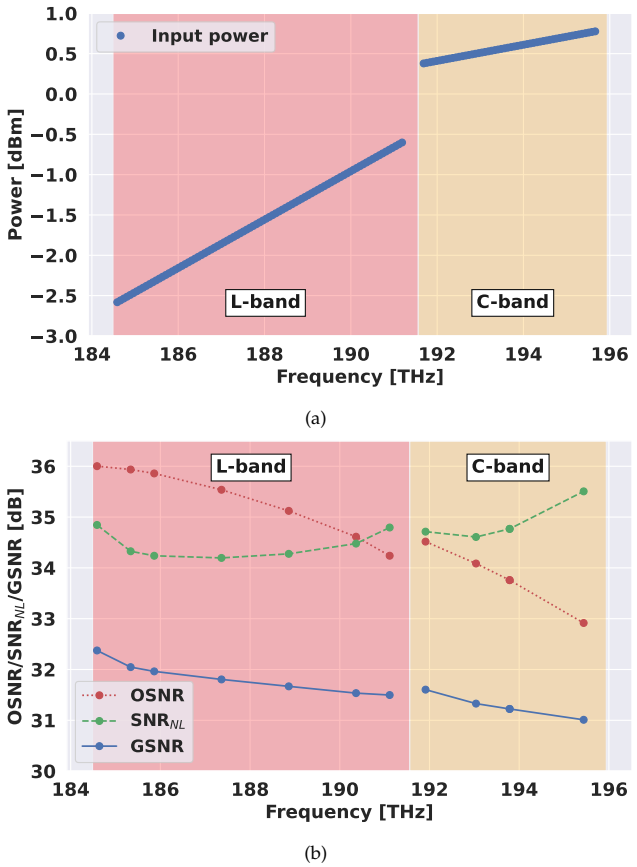

Fig. 4. Characteristics of the established C+L-band system, subject to upgrade in term of: (a) input power profile and (b) GSNR, OSNR and SNR$_{NL}$ of single 60 km span.

For this reason, we should consider a design optimized for this particular setup, which is characterized in Fig. 4 for a single span of 60 km. For a C+L-band system, we use the approach proposed in [27, 28], applying a tilt and offset to the flat optimal input power per channel, shown in Fig. 4(a). The average input power levels are -1.62 and 0.58 dBm for L- and C-band, respectively. By decreasing the input power in the L-band and increasing in the C-band, this approach aims at a compensation of the NLI interaction raised mainly by the SRS effect between these bands for that particular case. Figure 4(b) presents the GSNR, OSNR and SNL$_{NL}$ for the input power shown in Fig. 4(a). In it, we can see two opposite behaviors caused by the SRS effect. In C-band the OSNR is lower, indicating that more gain is needed in order to recover the propagation loss, and the SNR$_{NL}$ is higher, indicating that more power is lost during the propagation, resulting in a less intense nonlinear interaction. The opposite effect can be observed in the L-band, which due to the SRS effect will receive power instead of losing it as the C-band, resulting in a higher OSNR than the SNR$_{NL}$. The minimum GSNR for L-band is around 31.5 dB while the minimum value for C-band is 31 dB, which are the values used by the network control plane to estimate the QoT in each span, and consequently for the entire lightpath. The results shown in Fig. 4 aim to highlight that adding more bands to transmission without equalizing the input powers considerably changes the nature of the QoT, between linear (lower OSNR than SNR$_{NL}$) and nonlinear (lower SNR$_{NL}$ than OSNR) and / or diminishing it. As we simulate a C+L-band system that has been already deployed, the next analysis assumes ~~that it is not possible to change~~ to keep unchanged the input powers in the C+L-band system reported in Fig. 4(a), in order to limit reconfigurations. Note that this work focuses on assessing the impact of adding one spectral band (S- or E-band) in QoT and quantifying network capacity enhancements for these network upgrade scenarios in Sec. 3. [We are assuming that the performance in the already deployed C+L-band cannot be degraded as consequence of the newly carried out upgrades.]

Following our analysis, in Fig. 5(a) we present the GSNR profile for all CUTs comparing three scenarios: (a) C+L-band ([red] circles), (b) C+L+S-band ([green] triangles) and (c) C+L+E-band ([blue] squares) with the GB = 14 THz spacing between C- and E-band, for a single span with length of 60 km. The input powers levels are 0.76 and 2.27 dBm per channel for S- and E-band, respectively, also for a 60 km long span, optimized considering fixed power levels in C+L. The 14 THz GB between the C and E-band has been shown in [6] as the bandwidth ~~with the smallest impact~~ guaranteeing low impact on the QoT on the current C+L band. Indeed, as shown in Fig. 3, the Raman gain efficiency peak is more intense around that frequency offset, while for a larger spectral distance it rapidly decreases. Setting such [redacted] (unused spectrum) [redacted] that channels in E will be spaced by channels in C by a wider spectral distance and, even if we can not achieve a completely isolation, due to the long tails of the Raman efficiency, this [redacted] is able to maintain a negligible interaction between the channels of E- and C-bands. Firstly, we confirm that using this spacing to realize a C+L+E-band solution, the impact on QoT is insignificant. The average degradation of the minimum GSNR, among all lengths of the span found in the network, is less than 0.17 dB. The GSNR varies from 24.5 to 28 dB in the E-band. Regarding [the] S-band upgrade, Fig. 5(a) highlights the impact (green triangles) in the minimum GSNR on C- and L-band. The degradation in minimum GSNR is 0.8 and 1.13 dB for C- and L-band, respectively. Moreover, the GSNR in S-band ranges from 25.5 up to 27.2 dB. Figure 5(b) presents the minimum GSNR versus span length, considering a variation from 30 to 60 km, which is the maximum span length of the network physical topology being considered. The values are shown per band/scenario. Analyzing C-band (red curves), all lengths computed presented a larger degradation in this band if the S-band is added to the already deployed C+L-band system, compared to upgrading with the E-band. Moreover, the difference is higher for small spans than for larger ones, showing a maximum degradation of around 0.92 dB. S-band upgrade degradation (green curves) presents the same behaviour with highest impact for smaller spans. The maximum degradation of 1.3 dB is obtained for 30 km. Furthermore, it is possible to observe that in this band the degradation of using the E-band upgrade is negligible for all computed lengths, with a maximum value of 0.2 dB. Comparing the QoT of E- and S-band, the difference in performance is almost constant, with an average of 1.5 dB. Even with the QoT higher performance of S-band, E-band can attain a comparable performance in terms of allocated capacity, as it enables us to exploit a larger bandwidth (i.e., more channels). Both the delivered capacity and the impact on already deployed C+L-band channels are analysed at a network level in Sec. 3.

Finally, Table 1 presents the average (among all network span lengths) GSNR-penalty for both upgrade scenarios shown in Fig. 5 and a third scenario, in which we made use of a smaller GB, thus increasing the number of channels in the E band for a total of 166 channels in this band. ~~we made use of extra 1.5 THz of bandwidth in E-band for a total of 166 channels in this band.~~

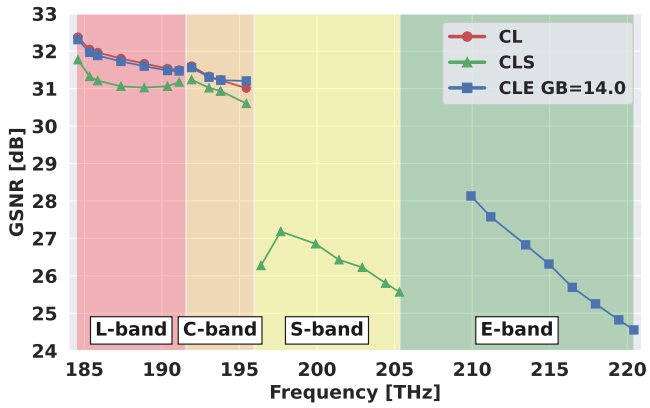

(a)

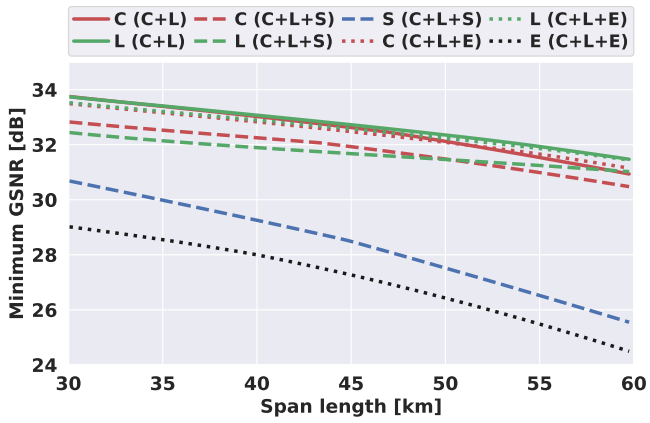

(b)

Fig. 5. (a) GSNR profile versus frequency for C+L-, C+L+E- and C+L+S-band and (b) Minimum GSNR per scenario (solid, dashed and dotted lines) per band (red, green, blue and black) versus span lengths.

Average Penalty	C+L+S	C+L+E (E=146 channels) GB = 14 THz	C+L+E (E=166 channels) GB = 12.5 THz
C-band	0.80 dB	0.17 dB	0.76 dB
L-band	1.13 dB	0.17 dB	0.65 dB

Table 1. Average GSNR penalty per band/scenario.

This third scenario adds more bandwidth, maintaining a more limited guard band presented in previous works [6]. It can be seen that adding the S-band or a wider E-band – but with a smaller GB – results in higher penalties if compared with the E-band with a guard-band of 14 THz. Note that the additional third scenario is added to evaluate whether, even with the higher GSNR penalties due to a more limited GB, the addition of 20 channels can have an improvement in reducing the network blocking probability. This is evaluated in Section 3.

Fig. 6. Spanish backbone topology.

3. NETWORK ANALYSIS

Upgrades to S- or E-band are compared by means of a custom-built event-driven C++ simulator. A 30-node Spanish backbone topology – shown in Fig. 6 – is considered. Traffic follows a Poisson distribution with $1/\lambda$ mean inter-arrival time. $1/\mu = 500$s is the mean connection holding time, exponentially distributed. Traffic load is expressed as λ/μ and it is varied up to 7500 Erlang by varying $1/\lambda$. Dual polarization quadrature phase shift keying (DP-QPSK) and dual polarization 16 quadrature amplitude modulation (DP-16QAM) are assumed with a symbol rate of 64 GBaud. 400-Gb/s-net-rate requests are considered. These requests can be routed using 1×400-Gb/s DP-16QAM signal occupying a 75 GHz frequency slot or via 2×200-Gb/s DP-QPSK signal to which a 150 GHz frequency slot is allocated. The GSNR of the worst channel (also considering cross-phase modulation) is assumed for each band. The following threshold values are assumed for GSNR to achieve a maximum pre-forward-error-correction bit error rate of 3×10^{-3} according to back-to-back transceiver characterization as in [29]: $\mathrm{TH}_{\mathrm{DP-16QAM}} = 16.1$ dB + M for DP-16QAM, $\mathrm{TH}_{\mathrm{DP-QPSK}} = 9.5$ dB + M for DP-QPSK, with M a parameter describing network margins (e.g., to account for aging [30]). Path computation is based on load balancing as in [31] and first fit policy within the chosen band is used for spectrum assignment. Regarding the choice of band, preference is given to the C-band; L-band is used when no spectrum continuity constraint can be satisfied in the C-band; S- or E-band are used when no spectrum continuity constraint can be satisfied in both C- and L-band. If the spectrum continuity constraint is not satisfied along C-, L-, and S- or E-band, the request is blocked.

Upgrades to S- and E-band are compared in terms of both blocking probability and the number of reconfigurations required to guarantee QoT in C+L-band when activating the new band. As described above, in the case of E-band upgrade, two GB (12.5 and 14.0 THz) between E- and C-band are considered.

Figure 7 shows the blocking probability versus traffic load of C+L-, C+L+S-, and C+L+E-band (with 12.5 THz and 14.0 THz of the GB between E- and C-band) with $M = 0$ (no margins). The exploitation of the S- or E-band results in a significant reduction in blocking probability. Moreover, the three different network upgrades provide a similar blocking probability. As an example, at a blocking of 10^{-2}, the exploitation of E- or S-band allows

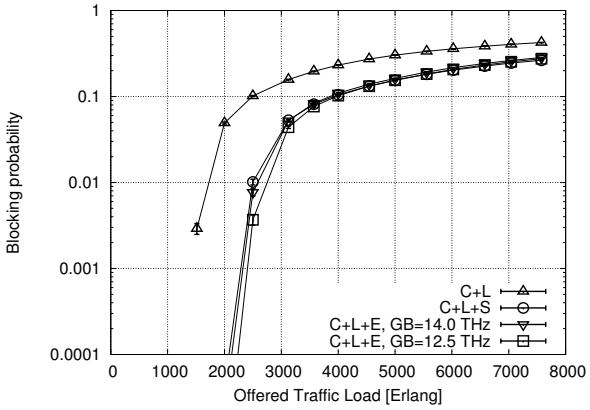

Fig. 7. Blocking probability versus traffic load with no margins

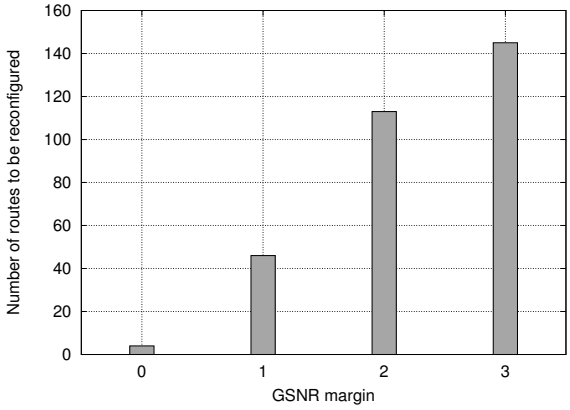

Fig. 8. Number of routes requiring reconfiguration when exploiting S-band versus margin M

us to support almost twice the traffic of the C+L-band. When comparing the upgrade to the S-band with the upgrade to the E-band with GB = 14.0 THz, although the latter exploits more spectrum (around 1.5 THz more), the GSNR in E-band results to be smaller than the one in the S-band (around 1 dB for a single span). This second effect translates into the more frequent use of lower-order modulation format, thus requiring more spectrum per request and balancing the presence of more spectrum in E-band. A similar effect is experienced when comparing the two different upgrades with the E-band, with GB = 12.5 THz and with GB = 14.5 THz, respectively. Indeed, E-band with smaller GB presents similar blocking than that with larger GB. On the one hand, upgrading to the E-band with GB = 12.5 THz offers more channels (1.5 THz of ~~spectrum more~~ → more spectrum), but from the other hand, GSNR with GB = 12.5 THz is lower than the one with GB = 14 THz (around 1 dB on a single span). This GSNR reduction is due to the presence of more channels when GB = 12.5 THz is adopted, resulting in a greater impact of nonlinear effects. Consequently, lower-order modulation formats are more widely used, resulting in a similar blocking probability despite the extra channels.

Moreover, it should be noticed that in some cases, the update may not be seamless, since several routes in the C+L-band require a reconfiguration because of the impact of SRS when a new band starts to be used. In particular, an impact is experienced on already active channels in C+L when the upgrade is done with S- or E-band and GB = 12.5 THz. On the contrary, as mentioned above, it has been observed that to bring up the E-band with GB = 14.0 THz does not imply any reconfiguration in the channels deployed in the C+L-band.

Figure 8 shows the number of routes requiring reconfigurations (e.g., re-routing, modulation format change, bit rate reduction) versus the margin value M when an upgrade to the S-band is adopted. Note that the present simulations are assuming – in the case of reconfiguration – a change of the modulation format (always from DP-16QAM to DP-QPSK) with a bit rate reduction; alternatively, additional channels should be established to preserve the original bit rate. With no margins ($M = 0$), 4 out of 870 routes require reconfigurations in C+L-band channels when using the S-band. The number of routes to be reconfigured increases with M since QoT requirements become more stringent. Consequently, more routes are critical, with a GSNR close to the

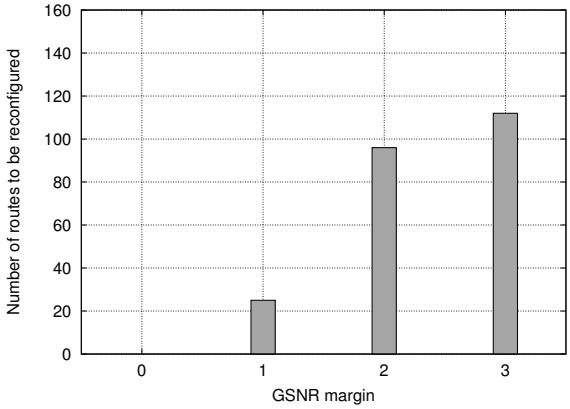

Fig. 9. Number of routes requiring reconfiguration when exploiting E-band with GB=12.5 THz versus margin M

threshold such that the GSNR variation due to SRS brings it below $\mathrm{TH}_{\mathrm{DP-16QAM}}$. As an example, with $M = 1$ dB, the channels along more than 40 routes would need to be reconfigured. ~~with $M = 2$ dB, the channels along around 113 routes would need to be reconfigured.~~

The upgrade to E-band with GB = 12.5 THz may also induce reconfigurations in C+L-band, as shown in Fig. 9. Although with $M = 0$, channels do not need reconfiguration in the assumed scenario, some reconfigurations are required when increasing the margin. As an example, with $M = 1$ dB, channels along more than 20 routes would need to be reconfigured. ~~As an example, with $M = 2$ dB, channels along around 96 routes would need to be reconfigured.~~ By comparing Fig. 8 and Fig. 9, it is clear that upgrading to S-band induces more reconfigurations in C+L-band than the upgrade to E-band with GB = 12.5 THz.

Figure 10 shows the blocking probability versus M at a load of 2500 Erlang. As expected, the blocking probability increases with M, since QoT becomes more stringent, translating into the use of the less spectral efficient DP-QPSK format, which demands more spectrum (150 GHz instead of 75 GHz). For

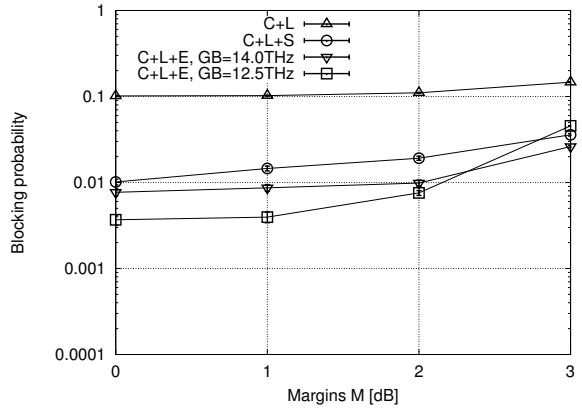

Fig. 10. Blocking probability versus margin M at a load of 2500 Erlang

the load considered, upgrading to E-band with GB = 12.5 THz experiences slightly better performance than the others until the margins are limited ($M \leq 2$ dB). With $M = 3$, upgrade to E-band with GB = 12.5 THz presents slightly worse performance. Indeed, on the one hand, with that GB value, GSNR in the E-band presents lower value (e.g., with respect to GB= 14.0 THz), given that SRS cannot be neglected. From the other side, $M =$ 3 dB drives ~~an~~ a high threshold on GSNR. Thus, this combination of lower GSNR and high threshold requires that the DP-QPSK is more frequently used. Consequently, more spectrum is occupied and, thus, higher blocking is experienced.

4. CONCLUSIONS

We compared network upgrades that exploit the S- or E-band taking into account Stimulated Raman Scattering, assuming the availability of amplifiers, filters, and interfaces compatible with these bands. Network simulations have shown that an upgrade to the E-band while relying on a properly selected guard band between E- and C-band may be preferred to an upgrade to the S-band. Indeed, on the one hand, upgrade scenarios exploiting the E- or S-band achieve similar traffic increment (e.g., almost double traffic with the E-band with respect to the original C+L-band system). On the other hand, the upgrade to E-band when a guard band is properly designed (GB = 14.0 THz in the considered scenario) does not imply any channel reconfiguration in C+L-band (e.g., modulation format adaptation), while the upgrade to S-band or to E-band with GB = 12.5 THz may impact QoT in C+L-band to such an extent that channel reconfigurations are required. ~~, especially when high network margins are adopted.~~ Future works may investigate network upgrades and re-configurations in the presence of more advanced transmission systems, such as probabilistic constellation shaping, which provides finer trade-offs between optical reach and spectral efficiency.

5. ACKNOWLEDGEMENT

This work was partially funded by Marie Skłodowska-Curie ITN MENTOR (GA 956713) and ETN WON (GA 814276). Lawrence Livermore National Laboratory is operated by Lawrence Livermore National Security, LLC, for the U.S. Department of Energy, National Nuclear Security Administration under Contract DE-AC52-07NA27344. LLNL-JRNL-835179. A. Napoli, J. Pedro and N. Costa would like to thank the European Commission for funding their activities through the H2020 B5G-OPEN (G.A. 101016663).

REFERENCES

1. A. Ferrari, A. Napoli, J. K. Fischer, N. Costa, J. Pedro, N. Sambo, E. Pincemin, B. Sommerkohrn-Krombholz, and V. Curri, "Upgrade capacity scenarios enabled by multi-band optical systems," in 2019 21st International Conference on Transparent Optical Networks (ICTON), (IEEE, 2019), pp. 1–4.
2. N. Sambo, A. Ferrari, A. Napoli, N. Costa, J. Pedro, B. Sommerkorn-Krombholz, P. Castoldi, and V. Curri, "Provisioning in multi-band optical networks," IEEE/OSA JLT **38**, 2598–2605 (2020).
3. A. Ferrari, A. Napoli, J. K. Fischer, N. Costa, A. D'Amico, J. Pedro, W. Forysiak, E. Pincemin, A. Lord, A. Stavdas, J. P. F.-P. Gimenez, G. Roelkens, N. Calabretta, S. Abrate, B. Sommerkorn-Krombholz, and V. Curri, "Assessment on the achievable throughput of multi-band ITU-T G.652.D fiber transmission systems," J. Light. Technol. **38**, 4279–4291 (2020).
4. R. Schmogrow, "Solving for scalability from multi-band to multi-rail core networks," J. Light. Technol. **40**, 3406–3414 (2022).
5. "Windstream deploys infinera C+L solution, sets foundation to double fiber capacity, url= https://www.infinera.com/press-release/windstream-deploys-infinera-c-lsolution-sets-foundation-double-fiber-capacity," .
6. N. Sambo, A. Ferrari, A. Napoli, J. Pedro, L. S. Kiani, P. Castoldi, and V. Curri, "Multiband Seamless Network Upgrade by Exploiting the E-band," in 2021 European Conference on Optical Communication (ECOC), vol. Tu2E.1 (IEEE, 2021), pp. 1–4.
7. N. Sambo, B. Correia, A. Napoli, J. Pedro, P. Castoldi, and V. Curri, "Transport network upgrade exploiting multi-band systems: S- versus E-band," in 2022 Optical Fiber Communications Conference and Exhibition (OFC), (2022), pp. 1–3.
8. R. Sadeghi, B. Correia, A. Souza, N. M. S. d. Costa, J. Pedro, A. Napoli, and V. Curri, "Transparent vs translucent multi-band optical networking: Capacity and energy analyses," J. Light. Technol. pp. 1–1 (2022).
9. F. Boubal, E. Brandon, L. Buet, S. Chernikov, V. Havard, C. Heerdt, A. Hugbart, W. Idler, L. Labrunie, P. Le Roux, S. Lewis, A. Pham, L. Piriou, R. Uhel, and J.-P. Blondel, "4.16 Tbit/s (104 /spl times/ 40 Gbit/s) unrepeatered transmission over 135 km in S+C+L bands with 104 nm total bandwidth," in Proceedings 27th European Conference on Optical Communication (Cat. No.01TH8551), vol. 1 (2001), pp. 58–59 vol.1.
10. H. Thiele, L. Molle, R. Freund, H.-J. Tessmann, D. Breuer, W. Jacobi, and M. Arbore, "40-gb/s S-band WDM transmission over installed fiber links using erbium-based fiber amplifiers," in OFC/NFOEC Technical Digest. Optical Fiber Communication Conference, 2005., vol. 2 (2005), pp. 3 pp. Vol. 2–.
11. S. Aozasa, H. Masuda, H. Ono, T. Sakamoto, T. Kanamori, Y. Ohishi, and M. Shimizu, "1480-1510 nm-band Tm doped fiber amplifier (TDFA) with a high power conversion efficiency of 42 %," in Proc. of OFC, (2001).
12. "S-band optical amplifier (TDFA) by FiberLabs, url=https://www.fiberlabs.com/bt_amp_index/s-band-bt-amp/," .
13. E. Dianov, "Bismuth-doped optical fibers: a challenging active medium for near-IR lasers and optical amplifiers," Light. Sci. & Appl. **1** (2012).
14. J. W. Dawson and et al., "E-band Nd 3+ amplifier based on wavelength selection in an all-solid micro-structured fiber," Opt. express **25**, 6524–6538 (2017).
15. "Waveshaper, url=https://ii-vi.com/product-category/products/optical-communications/optical-instrumentation/," .
16. R. Kraemer, F. Nakamura, M. v. d. Hout, S. van der Heide, C. Okonkwo, H. Tsuda, A. Napoli, and N. Calabretta, "Multi-band photonic integrated wavelength selective switch," J. Light. Technol. **39**, 6023–6032 (2021).
17. N. Fontaine, M. Mazur, R. Ryf, H. Chen, L. Dallachiesa, and D. Neilson, "36-THz bandwidth wavelength selective switch," in Proc. of ECOC, (2021).

18. N. Deng, L. Zong, H. Jiang, Y. Duan, and K. Zhang, "Challenges and enabling technologies for multi-band WDM optical networks," J. Light. Technol. pp. 1–1 (2022).
19. G. Di Rosa, R. Emmerich, M. Ribeiro Sena, J. K. Fischer, C. Schubert, R. Freund, and A. Richter, "Characterization, monitoring, and mitigation of the I/Q imbalance in standard c-band transceivers in multi-band systems," J. Light. Technol. pp. 1–1 (2022).
20. M. Cantono, D. Pilori, A. Ferrari, C. Catanese, J. Thouras, J.-L. Augé, and V. Curri, "On the interplay of nonlinear interference generation with stimulated raman scattering for qot estimation," J. Light. Technol. **36**, 3131–3141 (2018).
21. M. Nakagawa, H. Kawahara, K. Masumoto, T. Matsuda, and K. Matsumura, "Performance evaluation of multi-band optical networks employing distance-adaptive resource allocation," in 2020 Opto-Electronics and Communications Conference (OECC), (2020).
22. M. Mehrabi, H. Beyranvand, and M. J. Emadi, "Multi-band elastic optical networks: Inter-channel stimulated raman scattering-aware routing, modulation level and spectrum assignment," J. Light. Technol. **39**, 3360–3370 (2021).
23. F. Calderón, A. Lozada, P. Morales, D. Bórquez-Paredes, N. Jara, R. Olivares, G. Saavedra, A. Beghelli, and A. Leiva, "Heuristic approaches for dynamic provisioning in multi-band elastic optical networks," IEEE Commun. Lett. **26**, 379–383 (2022).
24. V. Kamalov and et al., "The subsea fiber as a Shannon channel," in In Proceedings of the SubOptic, (2019).
25. V. Curri, "Software-defined WDM optical transport in disaggregated open optical networks," in ICTON 2020, (IEEE, 2018), p. We.C2.1.
26. A. Ferrari, M. Filer, K. Balasubramanian, Y. Yin, E. Le Rouzic, J. Kundrát, G. Grammel, G. Galimberti, and V. Curri, "GNPy: an open source application for physical layer aware open optical networks," J. Opt. Commun. Netw. **12**, C31 (2020).
27. A. Ferrari, D. Pilori, E. Virgillito, and V. Curri, "Power Control Strategies in C+L Optical Line Systems," 2019 Opt. Fiber Commun. Conf. Exhib. OFC 2019 - Proc. pp. 10–12 (2019).
28. B. Correia, R. Sadeghi, E. Virgillito, A. Napoli, N. Costa, J. Pedro, and V. Curri, "Power control strategies and network performance assessment for C+L+S multiband optical transport," J. Opt. Commun. Netw. **13**, 147 (2021).
29. A. Nespola, S. Straullu, A. Carena, G. Bosco, R. Cigliutti, V. Curri, P. Poggiolini, M. Hirano, Y. Yamamoto, T. Sasaki, J. Bauwelinck, K. Verheyen, and F. Forghieri, "Gn-model validation over seven fiber types in uncompensated pm-16qam nyquist-wdm links," IEEE Photonics Technol. Lett. **26**, 206–209 (2014).
30. P. Soumplis, K. Christodoulopoulos, M. Quagliotti, A. Pagano, and E. Varvarigos, "Network planning with actual margins," IEEE/OSA JLT **35**, 5105–5120 (2017).
31. N. Sambo, F. Cugini, G. Bottari, P. Iovanna, and P. Castoldi, "Distributed setup in optical networks with flexible grid," in 2011 37th European Conference and Exhibition on Optical Communication, (2011), pp. 1–3.